AIP | Review of Scientific Instruments

Spatially confined low-power optically pumped ultrafast synchrotron x-ray nanodiffraction

Joonkyu Park, Qingteng Zhang, Pice Chen, Margaret P. Cosgriff, Jack A. Tilka, Carolina Adamo, Darrell G. Schlom, Haidan Wen, Yi Zhu, and Paul G. Evans

Citation: Review of Scientific Instruments **86**, 083904 (2015); doi: 10.1063/1.4929436
View online: http://dx.doi.org/10.1063/1.4929436
View Table of Contents: http://scitation.aip.org/content/aip/journal/rsi/86/8?ver=pdfcov
Published by the AIP Publishing

Spatially confined low-power optically pumped ultrafast synchrotron x-ray nanodiffraction

Joonkyu Park,[1] Qingteng Zhang,[1] Pice Chen,[1,a)] Margaret P. Cosgriff,[1] Jack A. Tilka,[1] Carolina Adamo,[2] Darrell G. Schlom,[2,3] Haidan Wen,[4] Yi Zhu,[4] and Paul G. Evans[1,b)]
[1]*Department of Materials Science and Engineering and Materials Science Program, University of Wisconsin-Madison, Madison, Wisconsin 53706, USA*
[2]*Department of Materials Science and Engineering, Cornell University, Ithaca, New York 14853, USA*
[3]*Kavli Institute at Cornell for Nanoscale Science, Ithaca, New York 14853, USA*
[4]*X-ray Science Division, Argonne National Laboratory, Argonne, Illinois 60439, USA*

(Received 13 June 2015; accepted 11 August 2015; published online 27 August 2015)

The combination of ultrafast optical excitation and time-resolved synchrotron x-ray nanodiffraction provides unique insight into the photoinduced dynamics of materials, with the spatial resolution required to probe individual nanostructures or small volumes within heterogeneous materials. Optically excited x-ray nanobeam experiments are challenging because the high total optical power required for experimentally relevant optical fluences leads to mechanical instability due to heating. For a given fluence, tightly focusing the optical excitation reduces the average optical power by more than three orders of magnitude and thus ensures sufficient thermal stability for x-ray nanobeam studies. Delivering optical pulses via a scannable fiber-coupled optical objective provides a well-defined excitation geometry during rotation and translation of the sample and allows the selective excitation of isolated areas within the sample. Experimental studies of the photoinduced lattice dynamics of a 35 nm $BiFeO_3$ thin film on a $SrTiO_3$ substrate demonstrate the potential to excite and probe nanoscale volumes. © *2015 AIP Publishing LLC.* [http://dx.doi.org/10.1063/1.4929436]

I. INTRODUCTION

Ultrafast phenomena in materials can be excited by optical pulses with durations of femtoseconds to picoseconds, an excellent match for the characteristic timescales of processes relevant to materials processing and fundamental physical phenomena. Time-resolved x-ray diffraction methods enable the study of the physics of condensed matter systems, including ultrafast laser-induced lattice dynamics of oxide materials,[1–4] semiconductor lattice dynamics,[5,6] and the metal-insulator transition in VO_2.[7] Several physical mechanisms result in the coupling of optical excitation to structural phenomena. The rapid thermalization of electron-hole pairs excited by an optical pulse produces rapid local thermal expansion and leads to coherent phonon emission.[5,8] Other mechanisms include the interaction between electrical polarization and excited charge carriers.[1] In the functional properties of complex oxide materials such as bismuth ferrite, $BiFeO_3$ (BFO), a lattice expansion of on the order of 0.1% can be induced by ultrafast above-bandgap optical excitation.[1,2,4,14] Beyond condensed matter physics, ultrafast optical pulses are widely used in the discovery and application of advanced methods for materials processing in field evaporation driven by local heating,[9] laser ablation,[10–12] and laser structuring.[13] Time-resolved x-ray diffraction experiments provide insight into structural effects by probing the optically induced variation in lattice parameters and symmetry, via resonant or non-resonant magnetic scattering, or through changes in unit-cell scale structure via the variation in the intensity of x-ray reflections resulting from changes in the structure function.

The size of the optical pump beam in optical pump/x-ray probe experiments is often chosen to match or exceed the size of the footprint of the x-ray beam in order to ensure that the x-ray diffraction information is derived only from the optically excited volume. The development of Fresnel zone plates, Kirkpatrick-Baez mirrors, and other x-ray nanofocusing optics now permits the creation of x-ray beams with spot sizes on the order of tens to hundreds of nanometers at synchrotron light sources.[15–17] The small x-ray spot size of diffraction instruments based on such focused beams promises to allow the study of individual optically excited nanometer-scale objects, or of the heterogeneous dynamics within larger samples. Previous applications of time-resolved nanobeam diffraction include nanosecond ferroelectric polarization domain dynamics,[18] the production of short-duration extremely large piezoelectric strain in $Pb(Zr,Ti)O_3$,[19] in which the temporal resolution was limited by the few-ns electric field risetime. Accessing shorter timescales requires the integration of ultrafast optical techniques with nanoscale x-ray probe beams.

The use of submicron x-ray beams in optical pump/x-ray probe experiments permits optical excitation schemes to be redesigned to distribute the illumination over only a small size matching the extent of the focused x-ray beam. We show here that a focused optical beam can be used to confine the optical radiation to an area close to the optical diffraction limit, creating a well-defined localized transient excitation. In addition, this scheme also reduces the total optical power and improves the thermal stability of the x-ray experiment. The optical fluences required for condensed matter physics and materials science experiments range from several mJ/cm^2 for

a)Present address: Department of Materials Science and Engineering, Northwestern University, Evanston, Illinois 60208, USA.
b)Electronic mail: pgevans@wisc.edu

non-destructive studies of optically induced transients[1,2,9,13] to several J/cm^2 for ablation, machining, and surface structuring.[10–12] The capability to create fluences reaching at least the lower end of this range is thus important in studies of electronic phenomena in solids. The scheme presented here produces focused optical beams in this mJ/cm^2 range.

We describe an instrument allowing tightly focused optical beams with lateral extents of a few microns to be combined with x-ray nanodiffraction instrumentation. The optical excitation is delivered to the sample using a single-mode optical fiber coupled to a high-numerical-aperture (NA) ultraviolet (UV) objective lens. The optical objective lens is mounted on a set of translation stages carried by the same translation and rotation stages as the sample. The optomechanical arrangement described here allows mechanical stability sufficient for x-ray nanobeam experiments. The optical geometry is decoupled from the rotation of the sample by the x-ray diffractometer so that the incident optical beam direction, along the surface normal in the present case, is constant throughout the experiment. As we show below, a low optical power of on the order of 10 μW can be used to produce a fluence of 1 mJ/cm^2 at experimentally useful repetition rates of tens of kHz. To reach similar optical fluences with more conventional 500 μm-scale optical beams would require total power of on the order of 10 mW and would lead to time-average temperature increases of several K or more in the sample.

II. INSTRUMENTATION

The optical pump/x-ray probe instrument is shown schematically in Fig. 1. There are three important aspects of the design and use of this instrument: (i) optical and x-ray focusing optics, (ii) optical focal spot characterization and alignment, and (iii) positioning of the sample and optical arrangement to permit two-dimensional x-ray diffraction mapping. Pulses produced by an ultrafast laser are coupled to a single-mode optical fiber and transmitted to the sample stage. The use of a single-mode optical fiber yields a focused beam with a well-defined spatial profile, which effectively improves the spatial resolution of experiments.

It is also informative to consider briefly the potential impact of the use of a multimode fiber to transfer the optical pulse to the sample stage. The modal dispersion that we estimate for the required 1 m length of typical commercial multimode fibers is on the order of tens of ps. The temporal broadening of the optical pulse resulting from the use of a multimode fiber would thus be much less than the 100 ps FWHM (full-width at half maximum) duration of x-ray pulses in the 24-bunch operating mode of the Advanced Photon Source (APS).[20,21] Using a multimode fiber would not cause the optical pulses to be longer than the typical x-ray bunch durations at synchrotron light sources, and our selection of a single-mode fiber is thus driven only by the simplification of the optical design afforded by the well-defined output of the single-mode fiber.

The optical beam exiting the fiber is collected by a collimator and focused into a micron-scale spot on the sample using an objective lens, as shown in Fig. 1. The optical beam is focused and translated laterally by a 3-axis objective translation stage (Attocube Systems AG) in order to overlap it with the footprint of the focused x-ray spot. Sample translation was achieved by mounting the sample and optical stages together on a 3-axis piezoelectric flexure scanning stage (nPoint, Inc.) which was in turn mounted on a 3-axis stepper-motor-driven coarse translation stage (MFN25PP, Newport, Inc.). All of these stages were mounted on a four-circle x-ray diffractometer to provide control of the orientation of the sample and the 2θ scattering angle.

A. Fiber coupling and focusing

The laser used in the experiment reported here (Duetto, Time-Bandwidth Products AG) produced 10 ps-duration output pulses at a fundamental wavelength of 1064 nm. The 1064 nm pulses were converted through third harmonic generation to a wavelength of 355 nm, corresponding to a photon energy of 3.49 eV. The experiments below required far less than the 5 W maximum output power available at 355 nm. The repetition rate of the optical pulses was locked to 1/5 of the orbital frequency of the APS, an optical pumping rate of 54 kHz. The laser repetition rate allowed time intervals of up to 18.5 μs to be studied following optical excitation before the re-excitation of the sample by a subsequent optical pulse.

The output of the laser was propagated in air to a fiber coupler (F-91-C1, Newport) consisting of an objective

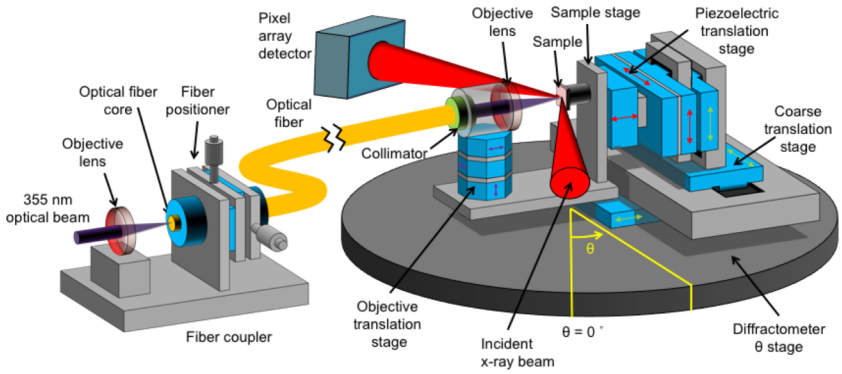

FIG. 1. Optical pump/x-ray nanoprobe instrument. An optical pulse with wavelength 355 nm is coupled into a single-mode optical fiber. The output of the fiber is collected by a collimator and focused by an objective lens onto the sample.

lens (U-27X, Newport, Inc.) and a 3-axis fiber positioner (FPR1-C1A, Newport, Inc.). The optical fiber (F-SM-300-SC, Newport, Inc.) had a single-mode wavelength range of 305–450 nm. The mode field diameter, specified as the diameter at which the field intensity is reduced to a factor of $1/e^2$ of its maximum,[22] is 3 μm. The numerical aperture of the coupling lens was 0.13 and the fiber has NA specified as 0.12–0.14. The output of the optical fiber was connected to a collimator (CFC-11X-A, ThorLabs, Inc.) with a focal length of 11 mm. The collimated optical pulse was focused onto the sample by an objective lens (UV0928, Universe Kogaku America, Inc.), with NA of 0.18, and front and back focal lengths of 8.995 and 11.075 mm, respectively. The working distance of the objective lens was 10.98 mm.

The optical power was measured at the output of the optical fiber in order to determine the coupling efficiency and thus to allow the experimental power to be selected. In a test with an incident optical power of 3.9 mW before fiber coupling, the output power was 75 μW, corresponding to a coupling efficiency of 2%.

B. Optical spot size characterization

The FWHM D of the focused spot laser on the sample surface can be found by computing the size of the image of the mode field diameter (w) of the fiber given above,[23]

$$D = \frac{\sqrt{2ln2}}{2} \times M \times w. \quad (1)$$

Here the magnification, M, is the ratio of the focal length of the collimator to the back focal length of the objective lens, a value of 1.01. Based on the optical parameters given above, we predict D = 1.8 μm, compared to the 50–500 μm size of optical pump beams employed in previous time-resolved diffraction experiments.

The size of the focused optical spot was measured by mounting an optical power meter on the sample stage as shown in Fig. 2(a). An opaque knife edge was used to block approximately half of the power meter. The focused laser was then scanned across the knife edge vertically by translating the objective lens and collimator. A measurement of the transmitted optical power as a function of the relative knife edge position in Fig. 2(b) gives a FWHM of 1.9 μm for the intensity of the focused optical beam.

The magnitude of the sample excitation is described using the absorbed fluence (F_a), defined as the optical fluence transmitted through the surface of the sample and absorbed within a thin film sample.[2] At normal incidence, F_a depends on the incident laser fluence (F_i), the optical refractive index of the sample (n), the optical absorption coefficient of the thin film (α), and the film thickness (Δ). With approximations that reflection at the substrate/film interface and nonlinear effects are negligible, the absorbed fluence is

$$F_a = F_i\left(1 - \left(\frac{n-1}{n+1}\right)^2\right)(1 - \exp(-\alpha\Delta)). \quad (2)$$

For BFO, n and α are 3.396 and 0.035 nm^{-1} at a wavelength of 355 nm.[24] For the present case of a film with thickness Δ = 35 nm, the absorbed fluence (F_a) is $0.49F_i$.

C. Time-resolved x-ray diffraction

The optical pump/x-ray probe system was characterized in a time-resolved x-ray nanodiffraction experiment at station 7-ID-C of the APS. The experiment probed the time dependence of the photoinduced strain following picosecond optical excitation of a BFO thin film. Previous studies have reported a significant expansion of the lattice of a BFO thin film following optical excitation, up to 0.44% within a time less than 100 ps for an absorbed fluence of 3.5 mJ/cm^2.[20,21] The samples for the studies reported here were the same 35 nm thick BFO film probed without spatial resolution in previous experiments.[1,2] The time dependence was investigated by varying the time interval between the x-ray pulses and the laser pulses.

Incident x-rays with a photon energy of 10 keV were focused to a spot on the sample using a Fresnel zone plate. The focused spot size in the vertical direction is 300 nm FWHM, and the diffraction geometry leads to a larger footprint of approximately 1 μm in the horizontal direction. Diffracted x-rays were detected by a pixel array detector (Pilatus 100 K, Dectris, Ltd.) gated to detect only diffracted x-ray intensity from pulses that arrive at a specified delay respect to the laser pulses. The detector was placed at nominal 2θ angle of 36.4° to

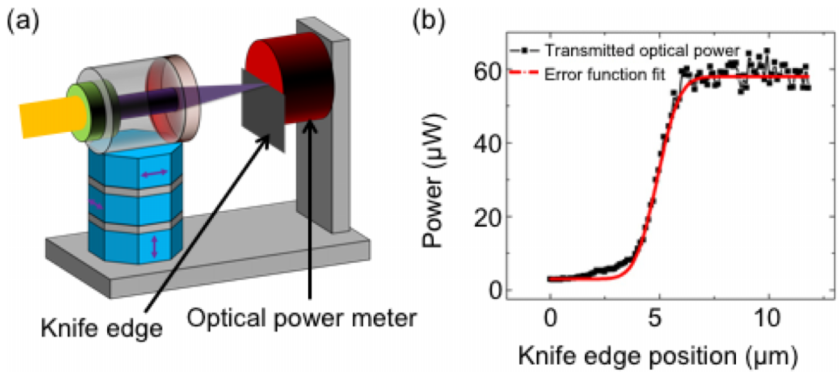

FIG. 2. (a) Optical spot size measurement by scanning the focused optical beam across a knife edge using the translation stage supporting the collimator and objective lens. (b) Transmitted optical power as a function of the vertical displacement of the laser relative to the knife edge. The full width at half maximum given by the error function fit (solid line) is 1.9 μm.

allow the pseudocubic 002 Bragg reflection of BFO to be studied. This experimental arrangement is depicted in Fig. 1. The area of interest on the thin film surface was chosen by moving the coarse sample translation stage to position the sample and optical focusing system with respect to the x-ray beam. Several one- or two-dimensional scans were used to search for positions where the x-ray and optical beams were overlapped. Micron-scale maps of the optical response were acquired by scanning the sample using the piezoelectric translation stage. The focused laser was then moved to the x-ray spot by manipulating the objective translation stage. The time-dependence of the response of the BFO following optical excitation was observed by varying the arrival time of the optical pulse relative to the fixed timing of the x-ray pulses. The delay time t is defined to be positive when the x-ray pulse arrives after the optical pulse and so that $t = T_0$ corresponds to the coincidence of x-ray and optical pulses.

III. RESULTS

The spatial variation and dynamics of optically induced effects as well as the overall stability of the instrument were evaluated in a series of experiments. Diffraction studies were undertaken to probe whether the response of small areas of the BFO film was consistent with what had been observed in earlier studies probing large areas of the sample. Rocking curve scans of the diffracted intensity of the specular BFO 002 x-ray reflection as a function of the x-ray incident angle θ are shown in Fig. 3 at values of the delay time corresponding to the arrival of the x-ray pulse before or after the optical pulse. The rocking curve measurement in Fig. 3 comprised a series of angular steps, for which diffracted intensities were measured at two times, 0.4 ns before (black) and 0.17 ns after (red) the optical excitation. The Bragg angle associated with the maximum intensity of the 002 x-ray reflection of BFO shifted from 18.27° to 18.25° following optical excitation, corresponding to a lattice expansion along the out-of-plane direction of 0.11%. This is consistent with the previous results reached at an absorbed fluence approximately 1 mJ/cm^2.[1,2]

A map of the spatial variation of the structural distortion produced by the optical excitation was obtained by measuring the diffracted x-ray intensity at a fixed incident beam angle

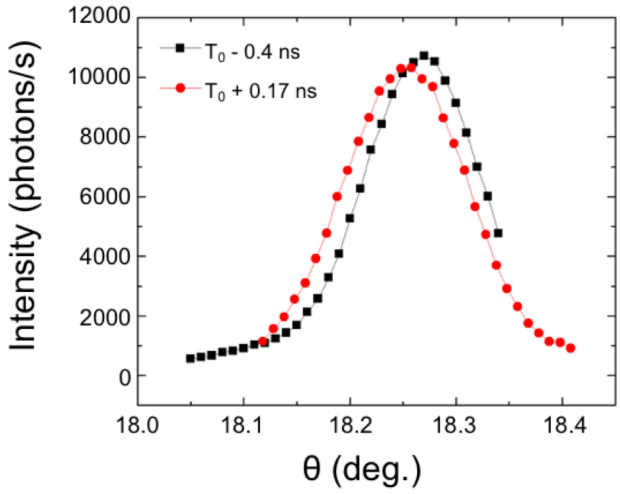

FIG. 3. Rocking curves of the intensity of the $BiFeO_3$ pseudocubic 002 Bragg reflection as a function of the incident x-ray beam angle. The diffracted x-ray intensity was measured with x-ray pulses arriving at times 0.4 ns before (black) and 0.17 ns after (red) the temporal coincidence of the optical and x-ray pulses, defined as time T_0. The scan at positive delay exhibits a peak shift from 18.27° to 18.25°, corresponding to an optically induced out-of-plane lattice expansion of 0.11%.

while rastering the sample position. The following procedure was used to assemble the diffraction maps shown in Fig. 4(a). The optical pump beam was set at a fixed location on the sample and the position of the sample and optical objective was scanned together with respect to the x-ray beam using the piezoelectric stage on which both were mounted, as shown in Fig. 1. This spatial map tests the thermal stability and spatial resolution of the instrument. The incident x-ray angle was fixed at $\theta = 18.20°$ during the spatial map, less than the steady-state Bragg angle $\theta = 18.27°$ of the BFO 002 reflection. Regions in which the lattice was expanded have the Bragg condition shifted to lower angle and thus appear brighter in intensity maps. The optically induced lattice expansion appears as a localized area of higher intensity in the diffracted intensity maps in Fig. 4(a) at time $t = +0.4$ ns, corresponding to a measurement at a time after the optical pulse. The x-ray and optical beams are overlapped at the location with high intensity in Fig. 4(a). The maximum intensity in the optically excited region in Fig. 4(a) was a factor of 1.2 larger than in

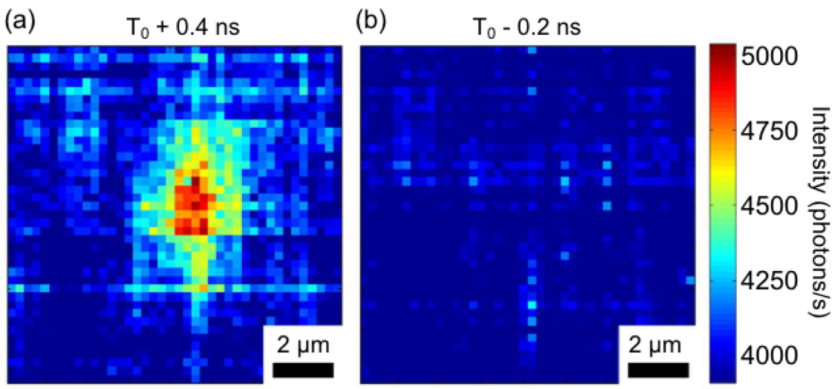

FIG. 4. Two-dimensional maps at times after and before T_0 at an x-ray incident angle of $\theta = 18.20°$, below the Bragg angle of 18.27°. (a) At positive delay, $T_0 + 0.4$ ns, the optically induced expansion leads to increased intensity in the central region of the map in which the optical pulse was focused. (b) At negative delay, $T_0 - 0.2$ ns, no photoinduced expansion is apparent.

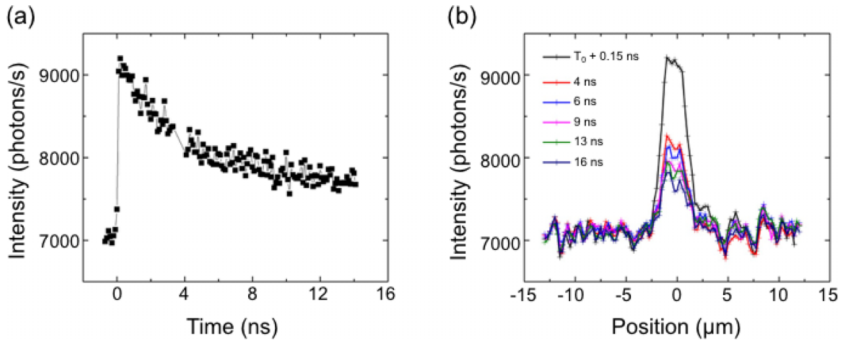

FIG. 5. (a) Delay scan acquired in the region of spatial overlap of the focused laser and x-ray pulses. (b) Spatial relaxation of the photoinduced lattice dynamics at various delay times from 0.15 ns to 16 ns.

the unilluminated region. The corresponding measurement at $t = -0.2$ ns in Fig. 4(b) represents the case in which the x-ray probe pulse arrives before the optical excitation and exhibits no optically induced perturbation. The photoinduced effect thus nominally recovered within the 18.5 μs interval between optical pulses.

The stability of the instrument was tested in two ways. First, the motion of features of higher or lower steady-state diffracted intensity in Fig. 4 is used to estimate the velocity with which the sample is moving with respect to the focused x-ray beam. Isolated regions producing higher or lower diffracted intensity can arise, for example, from structural artifacts due to epitaxial growth and are commonly observed in BFO thin films.[25] Local intensity variations in Figs. 4 and 5 were tracked between scans and the change in their positions between scans was used to estimate the drift of the x-ray focus with respect to the sample surface. The total shift in Fig. 4 was 0.5 μm during the 1.1 h interval between the scans, corresponding to a drift by 0.45 μm/h. A second estimate of the drift using the linear scans in Fig. 5 gives a velocity of 0.2 μm/h. We thus conclude that an upper limit for relative stability of the sample and focused laser beam during optical excitation is on the order of a several hundred nm/h.

A further study was conducted to probe the dynamics of the return of the BFO film to its steady-state lattice parameter at different places on the sample. The position of focused laser and x-ray was overlapped and a delay scan was performed at delay time from -1 ns to 14 ns. For these measurements, the absorbed fluence was 1 mJ/cm^2 and the incident x-ray angle was fixed at 0.06° below the steady-state Bragg angle of the BFO 002 reflection. As a result of the expansion, the intensity increased by a factor of 1.3 immediately following optical excitation, as shown in Fig. 5(a). The photoinduced perturbation decays over the period of several nanoseconds with a complex time dependence, initially falling by a factor of 2 within the first 4 ns, but persisting at a smaller level until at least 16 ns after excitation, as illustrated in Fig. 5(b). The initial rapid decay is associated with electronic phenomena and the slower decay persisting to the longest times measured in this study is associated with the slow relaxation of the thermal expansion of the film. A detailed thermal model is discussed in Ref. 2.

The spatial variation of the dynamics of the photoinduced excitation is shown in Fig. 5(b). The relative positions of the x-ray probe and optical excitation were scanned across a region 25 μm wide at delay times from 0.15 ns to 16 ns. The location of the optical excitation remained in a fixed position on the BFO surface. The time scale of the change in intensity agrees with the time dependence observed at a single point, as shown in Fig. 5(a). A key feature of the relaxation shown in Fig. 5(b) is that the lateral extent of the distorted region does not expand in the time following optical excitation, which is consistent with relatively large lateral scale of microns in comparison with the smaller 35 nm thickness of the film. The longitudinal sound velocity in BFO is 3.5 nm/ps, and thus, the propagation of the initial acoustic impulse through the thickness of the BFO layer is too fast to be captured with the time-resolution of this measurement.[4] The range of the scan in the lateral direction is sufficiently large to capture the acoustic transient, but no acoustic distortion is apparent in Fig. 5(b). We thus suspect that the distortion arising from the propagation of the acoustic impulse in the lateral direction is not sufficiently strong to be distinguished from the structural variation of the BFO layer.

IV. CONCLUSION

Combining ultrafast optical excitation with x-ray nanobeam diffraction enables the study of picosecond photoinduced structural dynamics in micron-scale excited regions. A micron-scale focused optical beam requires far lower power than unfocused optical excitation and thus thermal stability sufficient for synchrotron x-ray nanobeam experiments. Experiments with focused optical excitation show that the photoinduced dynamics in isolated regions of a BFO thin film sample are consistent with previous area-averaged measurements. More generally, the low optical power required to reach high fluences allows experiments to be conducted without heating large areas of the sample. The combination of a tightly focused optical pump with x-ray nanobeam diffraction has potential future applications in the characterization of the optical excitation of isolated regions within lithographically patterned structures and in the characterization of heterogeneous electronic materials.

ACKNOWLEDGMENTS

Work at the University of Wisconsin-Madison was supported by the U.S. DOE, Basic Energy Sciences, Materials

Sciences and Engineering, under Contract No. DE-FG02-04ER46147. Use of the Advanced Photon Source was supported by the U.S. Department of Energy, Office of Science, Office of Basic Energy Sciences, under Contract No. DE-AC02-06CH11357. H. W. and Y. Z. acknowledge support by the Argonne National Laboratory LDRD program under Grant No. 2013-036. Work at Cornell University was supported by the National Science Foundation (Nanosystems Engineering Research Center for Translational Applications of Nanoscale Multiferroic Systems) under Grant Number EEC-1160504. J.A.T. acknowledges support from the National Science Foundation Graduate Research Fellowship under Grant No. DGE-1256259.

[1]D. Schick, M. Herzog, H. D. Wen, P. Chen, C. Adamo, P. Gaal, D. G. Schlom, P. G. Evans, Y. L. Li, and M. Bargheer, Phys. Rev. Lett. **112**, 097602 (2014).
[2]H. D. Wen, P. Chen, M. P. Cosgriff, D. A. Walko, J. H. Lee, C. Adamo, R. D. Schaller, J. F. Ihlefeld, E. M. Dufresne, D. G. Schlom, P. G. Evans, J. W. Freeland, and Y. L. Li, Phys. Rev. Lett. **110**, 037601 (2013).
[3]D. Daranciang, M. Highland, H. Wen, S. Young, N. Brandt, H. Hwang, M. Vattilana, M. Nicoul, F. Quirin, J. Goodfellow, T. Qi, I. Grinberg, D. Fritz, M. Cammarata, D. Zhu, H. Lemke, D. Walko, E. Dufresne, Y. Li, J. Larsson, D. Reis, K. Sokolowski-Tinten, K. Nelson, A. Rappe, P. Fuoss, G. Stephenson, and A. Lindenberg, Phys. Rev. Lett. **108**, 087601 (2012).
[4]P. Ruello, T. Pezeril, S. Avanesyan, G. Vaudel, V. Gusev, I. C. Infante, and B. Dkhil, Appl. Phys. Lett. **100**, 212906 (2012).
[5]M. F. DeCamp, D. A. Reis, P. H. Bucksbaum, B. Adams, J. M. Caraher, R. Clarke, C. W. S. Conover, E. M. Dufresne, R. Merlin, V. Stoica, and J. K. Wahlstrand, Nature **413**, 825 (2001).
[6]A. Jurgilaitis, H. Enquist, B. P. Andreasson, A. I. Persson, B. M. Borg, P. Caroff, K. A. Dick, M. Harb, H. Linke, R. Nuske, L. E. Wernersson, and J. Larsson, Nano Lett. **14**, 541 (2014).
[7]A. Cavalleri, C. Tóth, C. W. Siders, J. A. Squier, F. Ráksi, P. Forget, and J. C. Kieffer, Phys. Rev. Lett. **87**, 237401 (2001).
[8]C. Thomsen, H. T. Grahn, H. J. Maris, and J. Tauc, Phys. Rev. B **34**, 4129 (1986).
[9]G. Sha, A. Cerezo, and G. D. W. Smith, Appl. Phys. Lett. **92**, 043503 (2008).
[10]E. G. Gamaly, N. R. Madsen, M. Duering, A. V. Rode, V. Z. Kolev, and B. Luther-Davies, Phys. Rev. B **71**, 174405 (2005).
[11]A. K. Sharma and R. K. Thareja, J. Appl. Phys. **98**, 033304 (2005).
[12]S. Tao, R. L. Jacobsen, and B. X. Wu, Appl. Phys. Lett. **97**, 181918 (2010).
[13]G. Heise, D. Trappendreher, F. Ilchmann, R. S. Weiss, B. Wolf, and H. Huber, J. Appl. Phys. **112**, 013110 (2012).
[14]B. Kundys, M. Viret, D. Colson, and D. O. Kundys, Nat. Mater. **9**, 803 (2010).
[15]F. Pfeiffer, C. David, J. F. van der Veen, and C. Bergemann, Phys. Rev. B **73**, 245331 (2006).
[16]C. G. Schroer, Phys. Rev. B **74**, 033405 (2006).
[17]H. Mimura, H. Yumoto, S. Matsuyama, Y. Sano, K. Yamamura, Y. Mori, M. Yabashi, Y. Nishino, K. Tamasaku, T. Ishikawa, and K. Yamauchi, Appl. Phys. Lett. **90**, 051903 (2007).
[18]A. Grigoriev, D.-H. Do, D. M. Kim, C.-B. E. eom, B. Adams, E. M. Dufresne, and P. G. Evans, Phys. Rev. Lett. **96**, 187601 (2006).
[19]A. Grigoriev, R. Sichel, H. N. Lee, E. C. Landahl, B. Adams, E. M. Dufresne, and P. G. Evans, Phys. Rev. Lett. **100**, 027604 (2008).
[20]T. Ejdrup, H. T. Lemke, K. Haldrup, T. N. Nielsen, D. A. Arms, D. A. Walko, A. Miceli, E. C. Landahl, E. M. Dufresne, and M. M. Nielsen, J. Synchrotron Radiat. **16**, 387 (2009).
[21]T. Graber, S. Anderson, H. Brewer, Y. S. Chen, H. S. Cho, N. Dashdorj, R. W. Henning, I. Kosheleva, G. Macha, M. Meron, R. Pahl, Z. Ren, S. Ruan, F. Schotte, V. Srajer, P. J. Viccaro, F. Westferro, P. Anfinrud, and K. Moffat, J. Synchrotron Radiat. **18**, 658 (2011).
[22]F. Mitschke, *Fiber Optics: Physics and Technology* (Springer, Heidelberg, 2010).
[23]Y. Zhao, H. Nakamura, and R. J. Gordon, Biomed. Opt. Express **1**, 1159 (2010).
[24]A. Kumar, R. C. Rai, N. J. Podraza, S. Denev, M. Ramirez, Y. H. Chu, L. W. Martin, J. Ihlefeld, T. Heeg, J. Schubert, D. G. Schlom, J. Orenstein, R. Ramesh, R. W. Collins, J. L. Musfeldt, and V. Gopalan, Appl. Phys. Lett. **92**, 121915 (2008).
[25]R. J. Sichel, A. Grigoriev, D. H. Do, S. H. Baek, H. W. Jang, C. M. Folkman, C. B. Eom, Z. H. Cai, and P. G. Evans, Appl. Phys. Lett. **96**, 051901 (2010).